Optik 125 (2014) 1550–1557

Contents lists available at ScienceDirect

Optik

journal homepage: www.elsevier.de/ijleo

New relationship of displacement signal at quadrant photodiode: Control signal analysis and simulation of a laser tracker

Žarko P. Barbarić[a], Stojadin M. Manojlović[b,*], Boban P. Bondžulić[b], Milenko S. Andrić[b], Srđan T. Mitrović[b]

[a] State University of Novi Pazar, Vuka Karadžića bb, 36000 Novi Pazar, Serbia
[b] University of Defence in Belgrade, Military Academy, Pavla Jurišića Šturma 33, 11000 Belgrade, Serbia

ARTICLE INFO

Article history:
Received 15 April 2013
Accepted 1 September 2013

Keywords:
Position sensitive detector
Quadrant photodiode
Displacement signal
Laser tracker simulation

ABSTRACT

New relationship of displacement signal using opposite sectors on a quadrant photodiode is derived. Standard and new displacement signals are analyzed in details. Through MATLAB® laser tracking simulation models, based on common and suggested approaches, detailed analysis is performed, and it is shown that better results for the new relationship signal processing are obtained. Within new relationship of displacement signal, the sensitivity of the system to the displacement of the spot increases and, hence, provides better accuracy in positioning up to 30%.

1. Introduction

Laser positioning systems have a special treatment, because their resolution is even better than resolution of radars. A number of applications of laser positioning systems include tracking of illuminated target and measurement of its angular position [1,2].

A precise determination of laser beam position or laser illuminated object position is provided using a quadrant photodiode. The quadrant photodiode (QPD) is a detector that consists of four separate photosensitive segments, separated by a gap or insensitive region. Because of its low noise, fast response, high sensitivity, ease of optical alignment, wide operating temperature range, and simple signal circuitry that follow up every QPD, it is one of the most commonly used position sensitive devices [3]. QPD is usually used in laser tracking and positioning [4–6], free-space optic communications [7], laser guided weapons [8], satellite communications, etc.

The principle of QPD positioning is simple. Incoming light is focused on the detector as a spot. Comparing of the output currents received from each of the four quadrants, the position of the spot on the surface can be determined. Thus, in general, photodetection system can be functionally divided into two main parts: a sensing stage and a post-processing one. In the second one, the signal post-processing stage, the standard approach for the control loop action of the servo system operates by the difference of the sum of signals coming from left- and right-side quadrants for horizontal and the difference of the sum of signals coming from upper- and down-side quadrants for vertical displacement [9].

This research suggests a new relationship of displacement signal using opposite sectors on a QPD. Efficiency of proposed approach is analyzed in detail and compared to standard approach. In a post-processing stage, through signal processing of signals from two opposite sectors on QPD – novel arrangement, the sensitivity of the detector to the displacement of the spot increases by a factor of about 1.4. Using the developed MATLAB® laser tracking simulation model it is shown that proposed sensitivity upgraded detector also provides better accuracy in positioning.

In the following, Section 2 introduces the standard signal post-processing stage. Proposed QPD signal combination is also outlined in Section 2. Simulation of a laser tracker is evaluated in Section 3, and the results are discussed in detail in Section 4.

* Corresponding author. Tel.: +381 60 303 2082.
E-mail addresses: barbaric@etf.rs (Ž.P. Barbarić), colemanojle@yahoo.com (S.M. Manojlović), bondzulici@yahoo.com (B.P. Bondžulić), asmilenko@beotel.rs (M.S. Andrić), srdjan.mitrovic@va.mod.gov.rs (S.T. Mitrović).

0030-4026/$ – see front matter © 2013 Elsevier GmbH. All rights reserved.
http://dx.doi.org/10.1016/j.ijleo.2013.10.012

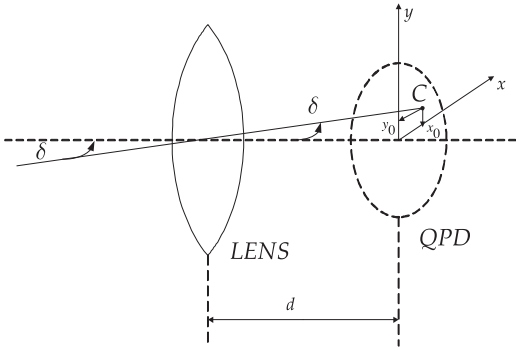

Fig. 1. A receiving lens and quadrant photodiode of a laser tracker.

2. Displacement signals

An optical part of a laser tracker with receiving lens and quadrant photodiode is shown in Fig. 1. The incoming laser energy and optical axis of a laser tracker form an angle δ. This angle is the displacement angle from optical axis of a laser tracker. The centre of laser spot $C(x_0, y_0)$ on QPD is a function of the angle δ. A relationship between components of angle δ, Fig. 1, in two orthogonal planes and the coordinates of the spot centre are: horizontal $\tan(\delta_h) = x_0/d$, and vertical $\tan(\delta_v) = y_0/d$, where d is the distance between the optical lens and the QPD.

Geometry of the QPD with a laser spot centred at (x_0, y_0) is shown in Fig. 2. Also, in Fig. 2 four segments and two coordinate systems are shown ($x0y$ and $\zeta 0\eta$). A direct measurement of displacements x_0 and y_0 by processing signals from the QPD is not possible. Firstly, a constant laser beam spot of radius r is assumed. Having the measured QPD current signals, it is possible to determine the ratios of displacements and a light spot radius, x_0/r and y_0/r. The spot surface in $x0y$ coordinate system is bounded by circle:

$$(x - x_0)^2 + (y - y_0)^2 = r^2 \tag{1}$$

The same equation in polar coordinates, from Fig. 2, is obtained by the substitutions $x = \rho\cos(\phi)$, $x_0 = \rho_0\cos(\phi_0)$, and $y = \rho\sin(\phi)$, $y_0 = \rho_0\sin(\phi_0)$ in a form of:

$$\rho^2 + \rho_0^2 - 2\rho\rho_0\cos(\phi - \phi_0) = r^2 \tag{2}$$

It is essential to know the irradiance distribution on the photodiode surface. If the irradiance on the photodiode surface is a constant, then the optical power on sector is $P_k = E_0 A_k$, where E_0 is the irradiance at the photodiode surface, and A_k is the area of the illuminated part of the kth sector or quadrant of the photodiode. Instead of current values acquired by QPD's kth sector, $I_k = \Re P_k$, where $\Re$ is photodiode conversion factor, areas of spot light that overlap with four quadrants, A_k, $k \in \{1, 2, 3, 4\}$ are used. In standard approach, the horizontal displacement signal ε_x is obtained from the difference of the areas from the left- and right-side quadrants. Analogously, the difference of the areas from the upper- and down-side quadrants defines the vertical displacement signal ε_y in Eq. (3) [1,2]. The power of the received signal is a function of the irradiance, laser power and atmospheric conditions, and the distance between a laser source and photodiode. These are the reasons for normalization of displacement signals. A normalized form of displacement signals for standard arrangement can be written for x, y orthogonal channels as:

$$\begin{aligned} \varepsilon_x &= \frac{(A_1 + A_4) - (A_2 + A_3)}{A_1 + A_2 + A_3 + A_4} \\ \varepsilon_y &= \frac{(A_1 + A_2) - (A_3 + A_4)}{A_1 + A_2 + A_3 + A_4} \end{aligned} \tag{3}$$

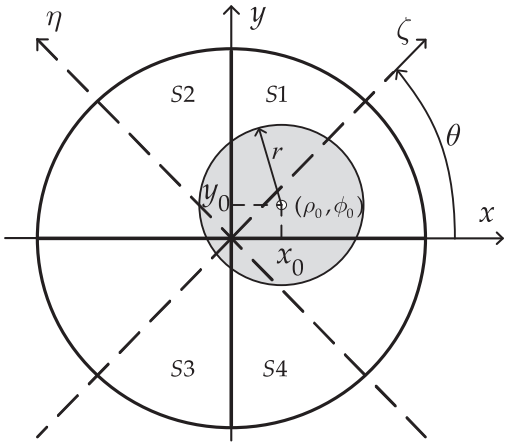

Fig. 2. Quadrant photodiode geometry.

The displacement signals along ζ and η axes are obtained from the difference of the signals received by the opposite sectors $S1$ and $S3$, and $S2$ and $S4$, respectively [10]. A normalized form of displacement signals for two opposite sectors in ζ, η orthogonal channels are:

$$\begin{aligned}\varepsilon_\zeta &= \frac{A_1 - A_3}{A_1 + A_3}\\ \varepsilon_\eta &= \frac{A_2 - A_4}{A_2 + A_4}\end{aligned} \tag{4}$$

The areas of the spot light that overlap with four quadrants, A_k (Eqs. (3) and (4)) can be calculated according to the double integral, (being given here for the sector $S1$):

$$A_1 = \int_0^{\pi/2}\int_0^{\rho(\phi)} \rho d\rho d\phi = \int_0^{\pi/2} \frac{(\rho(\phi))^2}{2} d\phi \tag{5}$$

where A_1 is the spot area in the first sector surface $S1$.

The radius ρ, in polar coordinates, is obtained from Eq. (2) in the form of:

$$\rho(\phi) = \rho_0 \cos(\phi - \phi_0) + \sqrt{(\rho_0 \cos(\phi - \phi_0))^2 - \rho_0^2 + r^2} \tag{6}$$

For sectors $S2$, $S3$ and $S4$, the limits of angle ϕ, as shown in Fig. 2, are respectively $[\pi/2, \pi]$, $[\pi, 3\pi/2]$ and $[3\pi/2, 2\pi]$.

The normalized form of displacement signals in the standard arrangement, marked with $(2-2)$ in superscript, along x and y axes are obtained according to the Eqs. (3) and (5) as:

$$\begin{aligned}\varepsilon_x(\rho_0, \phi_0) &= \frac{2}{\pi}\left(\frac{\rho_0}{r}\cos(\phi_0)\sqrt{1 - \left(\frac{\rho_0}{r}\cos(\phi_0)\right)^2} + \arcsin\left(\frac{\rho_0}{r}\cos(\phi_0)\right)\right)\\ \varepsilon_x(x_0) &= \frac{2}{\pi}\left(\frac{x_0}{r}\sqrt{1 - \left(\frac{x_0}{r}\right)^2} + \arcsin\left(\frac{x_0}{r}\right)\right) = \varepsilon_x^{(2-2)}, \quad |x_0| \le r\\ \varepsilon_y(\rho_0, \phi_0) &= \frac{2}{\pi}\left(\frac{\rho_0}{r}\sin(\phi_0)\sqrt{1 - \left(\frac{\rho_0}{r}\sin(\phi_0)\right)^2} + \arcsin\left(\frac{\rho_0}{r}\sin(\phi_0)\right)\right)\\ \varepsilon_y(y_0) &= \frac{2}{\pi}\left(\frac{y_0}{r}\sqrt{1 - \left(\frac{y_0}{r}\right)^2} + \arcsin\left(\frac{y_0}{r}\right)\right) = \varepsilon_y^{(2-2)}, \quad |y_0| \le r\end{aligned} \tag{7}$$

The normalized form of new displacement signals along ζ and η axes, according to Eqs. (4) and (5) are derived in the following way:

$$\begin{aligned}\varepsilon_\zeta(\rho_0, \phi_0) &= \frac{(\rho_0/r)\cos(\phi_0)\sqrt{1 - ((\rho_0/r)\cos(\phi_0))^2} + (\rho_0/r)\sin(\phi_0)\sqrt{1 - ((\rho_0/r)\sin(\phi_0))^2}}{(\pi/2) + (\rho_0^2/r^2)\sin(2\phi_0)} + \frac{a\sin((\rho_0/r)\cos(\phi_0)) + a\sin((\rho_0/r)\sin(\phi_0))}{(\pi/2) + (\rho_0^2/r^2)\sin(2\phi_0)}\\ \varepsilon_\zeta(x_0, y_0) &= \frac{(x_0/r)\sqrt{1 - (x_0/r)^2} + (y_0/r)\sqrt{1 - (y_0/r)^2} + a\sin(x_0/r) + a\sin(x_0/r)}{(\pi/2) + 2(x_0/r)(y_0/r)}\\ \varepsilon_\eta(\rho_0, \phi_0) &= \frac{(\rho_0/r)\sin(\phi_0)\sqrt{1 - ((\rho_0/r)\sin(\phi_0))^2} - (\rho_0/r)\cos(\phi_0)\sqrt{1 - ((\rho_0/r)\cos(\phi_0))^2}}{(\pi/2) - (\rho_0^2/r^2)\sin(2\phi_0)} + \frac{a\sin((\rho_0/r)\sin(\phi_0)) - a\sin((\rho_0/r)\cos(\phi_0))}{(\pi/2) - (\rho_0^2/r^2)\sin(2\phi_0)}\\ \varepsilon_\eta = \varepsilon_\eta(x_0, y_0) &= \frac{(y_0/r)\sqrt{1 - (y_0/r)^2} - (x_0/r)\sqrt{1 - (x_0/r)^2} + a\sin(y_0/r) - a\sin(x_0/r)}{(\pi/2) - 2x_0/r(y_0/r)}\end{aligned} \tag{8}$$

The standard displacement signals, Eq. (7), are functions of the corresponding coordinate of the spot centre (x_0 or y_0), but the new displacement signals, Eq. (8), are functions of both coordinates (x_0 and y_0). Both of them can be used as control signals in the laser tracker for dual-axes ($x-y$) positioning. The standard displacement signals given in Eq. (7) can be used directly, while displacement signals suggested in Eq. (8) have to be transformed in $x-y$ coordinate system. A relationship between displacement signals in two coordinate systems for $\theta = 45^\circ$, as shown in Fig. 2, is:

$$\begin{bmatrix}\varepsilon_x^{(1-1)}\\ \varepsilon_y^{(1-1)}\end{bmatrix} = \begin{bmatrix}\sqrt{2}/2 & -\sqrt{2}/2\\ \sqrt{2}/2 & \sqrt{2}/2\end{bmatrix} \cdot \begin{bmatrix}\varepsilon_\varsigma\\ \varepsilon_\eta\end{bmatrix} = T \cdot \begin{bmatrix}\varepsilon_\varsigma\\ \varepsilon_\eta\end{bmatrix} = \sqrt{2}/2 \begin{bmatrix}\dfrac{A_1 - A_3}{A_1 + A_3} - \dfrac{A_2 - A_4}{A_2 + A_4}\\ \dfrac{A_1 - A_3}{A_1 + A_3} + \dfrac{A_2 - A_4}{A_2 + A_4}\end{bmatrix} \tag{9}$$

where $\varepsilon_x^{(1-1)}$ and $\varepsilon_y^{(1-1)}$ are suggested displacement signals. The ratio of horizontal displacement signals for arrangements $(1-1)$ and $(2-2)$ is given by:

$$R_x = \frac{\varepsilon_x^{(1-1)}}{\varepsilon_x^{(2-2)}} \tag{10}$$

The normalized displacement signals $\varepsilon_x^{(2-2)}$ and $\varepsilon_x^{(1-1)}$ for three different values of $r_n = \rho_0/r$ are shown in Fig. 3, and their ratio R_x is shown in Fig. 4.

The displacement signal $\varepsilon_x^{(1-1)}$ has higher magnitude than signal $\varepsilon_x^{(2-2)}$ on the whole ϕ_0 range, for small values of r_n. The ratio R_x in Eq. (10) approaches $\sqrt{2}$ as the spot centre approaches the centre of QPD (Fig. 4 for $r_n = 0.1$), which indicates higher sensitivity of QPD using

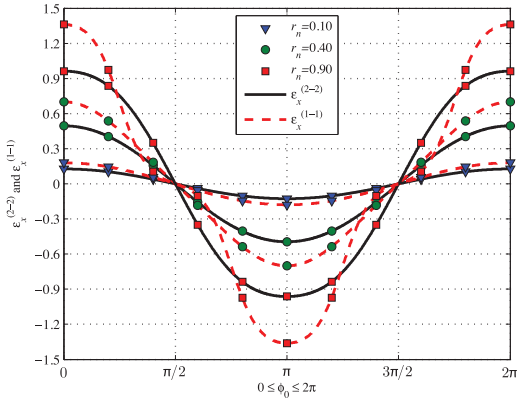

Fig. 3. The normalized displacement signals $\varepsilon_x^{(1-1)}$ and $\varepsilon_x^{(2-2)}$ as a function of ϕ_0, for $r_n = \rho_0/r \in \{0.1, 0.4, 0.9\}$.

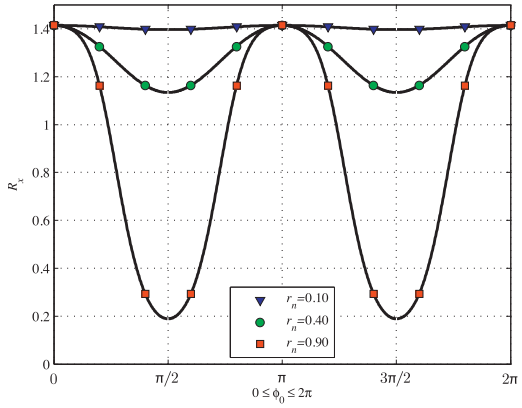

Fig. 4. Ratio of the normalized displacement signals $R_x = \varepsilon_x^{(1-1)}/\varepsilon_x^{(2-2)}$ as a function of ϕ_0, for $r_n \in \{0.1, 0.4, 0.9\}$.

$\varepsilon_x^{(1-1)}$ displacement signal [11]. The sensitivity of QPD, as error sensor, can significantly influence the control loop action of the servo system committed to the alignment operation [3,9,12]. The ratio R_y for vertical direction can be obtained in a similar way as R_x.

It is important to understand the way the displacement signals from different arrangements influence the dynamic characteristics of servo system. When ratio of displacement signals (R_x or R_y) is greater than 1, sensitivity of $(1-1)$ arrangement is higher than $(2-2)$, and the response of the servo system is faster [3]. As previously established, these ratios depend on spot centre position (r_n and ϕ_0) on QPD surface. In Fig. 5, the case when the sensitivity of the new arrangement is better than standard one in both directions ($R_x > 1$ and $R_y > 1$) is presented with dark grey color, approximately for $r_n < 0.5$ (dotted line in Fig. 5). Light grey area presents the cases where $R_x < 1$ and $R_y > 1$, or $R_x > 1$ and $R_y < 1$. White areas in Fig. 5 present the case when $R_x < 1$ and $R_y < 1$.

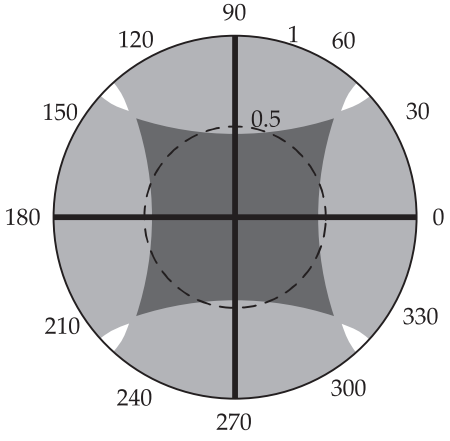

Fig. 5. Illustration of sensitivity for two arrangements in polar coordinates (r_n, ϕ_0).

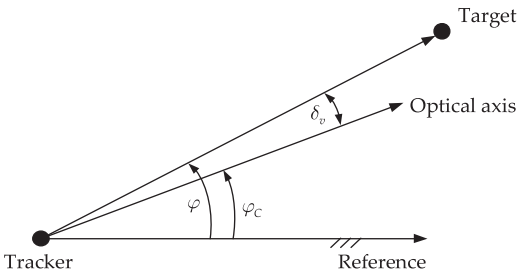

Fig. 6. Basic geometry in vertical plane for tracking system.

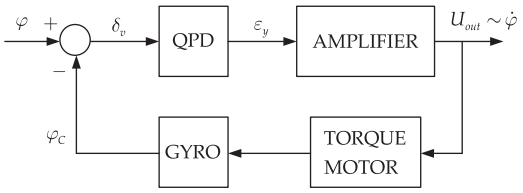

Fig. 7. A block diagram of a simple laser tracking system.

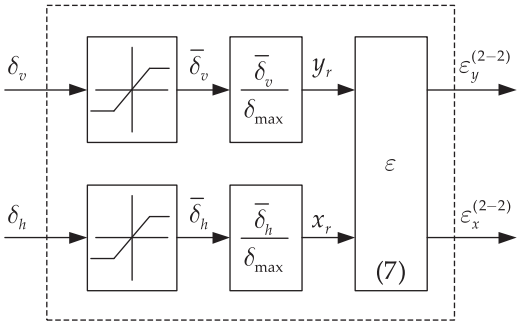

Fig. 8. Model of QPD for arrangement (2 – 2).

3. Simulation of a laser tracker

The displacement signals ε_x, ε_y and ε_ξ, ε_η are measures of target line of sight (LOS) and optical axis misalignment. Basic geometry in vertical plane for tracking system is shown in Fig. 6. A laser illumination energy comes to the receiving optics at the angle δ_v.

According to Fig. 6, the block diagram of a simple tracking system is presented in Fig. 7. The input signal φ represents LOS angle, φ_c stands for the angle of optical axis and δ_v is their angular displacement. The QPD provides a monotonously changing displacement signal ε_y within its tracking field of view (FOV). The signal U_{out} is proportional to the angular velocity of the LOS, $\dot{\varphi}$. The integration in the feedback path (GYRO) represents the angular motion of the receiver.

The QPDs models are proposed and presented in Figs. 8 and 9. Fig. 8 represents QPD model using standard displacement signals Eq. (7), and Fig. 9 represents QPD with suggested new form of displacement signals Eqs. (8) and (9).

Angles δ_v and δ_h are limited on $\pm\delta_{max}$, and if the angle error exceeds this value target tracking is not possible. The angles in the vertical and the horizontal planes, δ_v and δ_h correspond to normalized spot centre coordinates $x_r = x_0/r$ and $y_r = y_0/r$, respectively. Normalized coordinates are required for calculation of displacement signals, Eqs. (7) and (8).

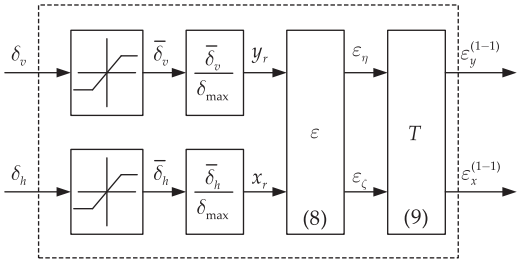

Fig. 9. Model of QPD for arrangement (1 – 1).

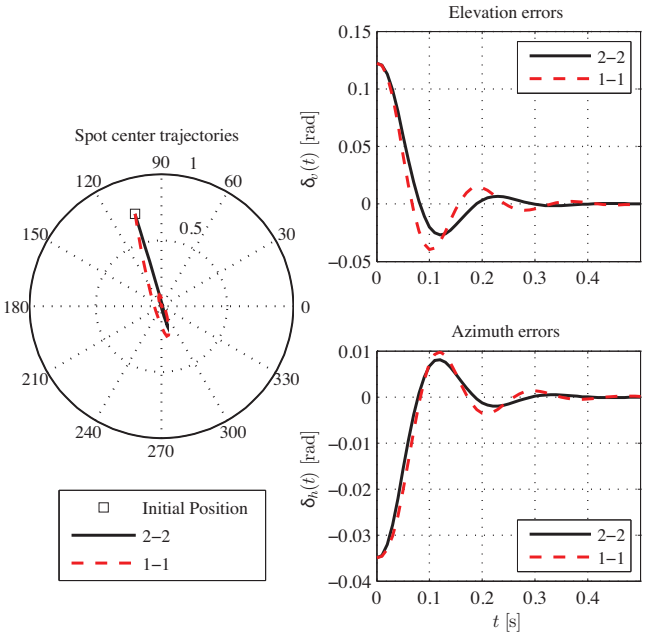

Fig. 10. Spot centre trajectories and angular errors for the Case 1.

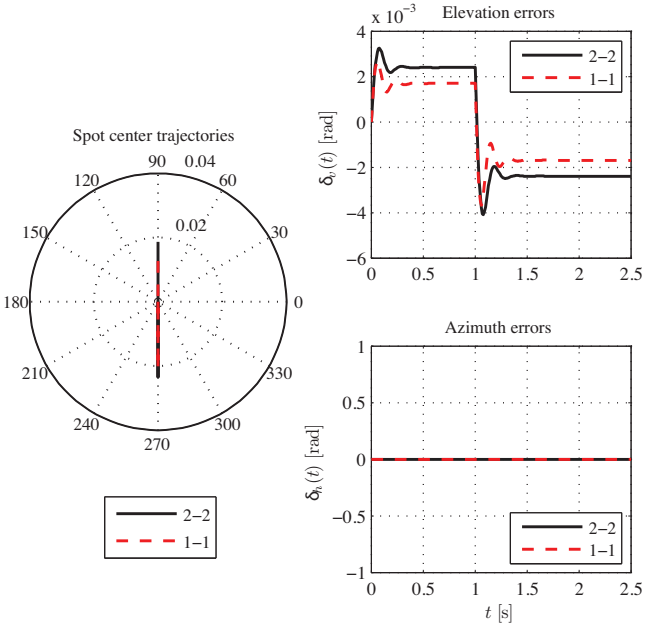

Fig. 11. Spot centre trajectories and angular errors for the Case 2.

4. Results analysis

A simulation of laser tracker, Fig. 7, with models of QPD, shown in Figs. 8 and 9, is provided through three cases, with stationary and moving targets. The influence of displacement signals from different arrangements on the dynamic characteristics of laser tracking servo system is analyzed.

4.1. Case 1 – Laser illuminated target is stationary one

In this case the target is a stationary one, with initial target position $x_r = -0.2$ ($\delta_h = -2^\circ = -0.035$ rad) and $y_r = 0.7$ ($\delta_v = 7^\circ = 0.122$ rad), in the sensor FOV ($\pm\delta_{max} = \pm 10^\circ$).

Fig. 10 shows initial position (marked as □) and trajectory of the centre of spot on QPD surface for both arrangements (left). The upper and bottom parts on the right of Fig. 10 show angular errors in vertical and horizontal planes for both arrangements. It can be seen that the laser tracker points to a stationary target with zero steady-state errors in vertical and horizontal planes, for both arrangements.

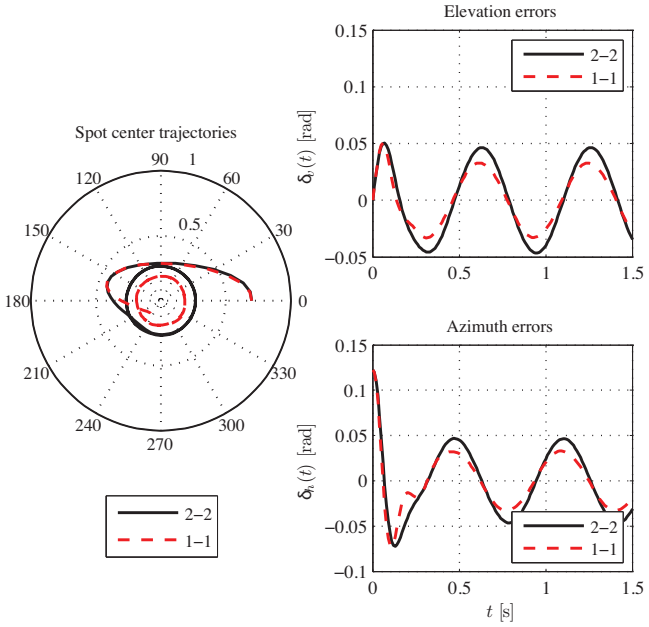

Fig. 12. Spot centre trajectories and angular errors for the Case 3.

4.2. Case 2 – Laser illuminated target moves in the vertical plane

In the second case, the target moves in the vertical plane. Initially, laser tracker points to target (optical axis and target LOS are collinear). At the beginning, the target goes up, and it changes direction after one second. The angular velocity of target LOS is $\dot{\varphi} = 4^\circ/\text{s}$. Fig. 11 shows spot centre trajectories and angular errors in the time.

As the target moves only in the vertical plane, the azimuth errors are zero, and it is shown in Fig. 11. The laser tracking system tracks a target with constant steady-state errors for both arrangements. The steady-state errors are inversely proportional to intensity of displacement signals, as expected according to [5]. In this case, the spot centre is always in the area where signals $\varepsilon_x^{(1-1)}$ and $\varepsilon_y^{(1-1)}$ are dominant (dark grey in Fig. 5), therefore in stationary regime, the accuracy of the laser tracker for suggested arrangement $(1-1)$ is better with ratio of approximately $\sqrt{2}$.

4.3. Case 3 – Laser illuminated target moves along the circle

In this case target LOS rotates with the constant angular velocity. Initially, the position of spot centre is $x_r = 0.7$ ($\delta_h = 7^\circ$=0.122 rad) and $y_r = 0$ ($\delta_v = 0$), in the sensor FOV ($\pm\delta_{max} = \pm 10^\circ$). Fig. 12 shows spot centre trajectories and angular errors in the time. The steady-state error oscillates around the zero due to circular trajectory of the target, as it is shown in Fig. 12. The laser tracking system tracks the target maintaining the spot centre in the area in the FOV, where the signals $\varepsilon_x^{(1-1)}$ and $\varepsilon_y^{(1-1)}$ are dominant. Therefore, the magnitude of the error signals in elevation and azimuth channels are lower for the suggested arrangement $(1-1)$.

5. Conclusion

A new relationship of displacement signal using opposite sectors on a QPD is derived. Based on new relationship the model of QPD is proposed. The simulation of laser tracker with common and new displacement signals as control signals is provided, and the accuracy of laser tracker system is analyzed.

The standard displacement signals in horizontal and vertical plane are independent, but the new normalized displacement signals along axes of rotated coordinate system are dependent on both spot centre coordinates. Through simple transformation, new displacement signals are adjusted for laser tracking. It has been shown that new displacement signal provides approximately $\sqrt{2}$ higher sensitivity of QPD, as the spot centre approaches the centre of QPD.

The common and new displacement signals have been used as control signals in the laser tracking system. Due to higher sensitivity, new displacement signals provide faster reaction of a laser tracker and tracking with better accuracy in steady-state (up to 30%), which was demonstrated by the simulations.

Acknowledgements

This paper has been partially supported by the Ministry of Education, Science and Technological Development, the Republic of Serbia under Grant TR-32023 and Project III-47029.

References

[1] A. Mäkynen, J. Kostamovaara, R. Myllylä, Positioning resolution of the position-sensitive detectors in high background illumination, IEEE Trans. Instrum. Meas. 45 (1) (1996) 324–326, http://dx.doi.org/10.1109/19.481361.

[2] L.M. Manojlovic, Z. Barbaric, Optimization of optical receiver parameters for pulsed laser-tracking systems, IEEE Trans. Instrum. Meas. 58 (3) (2009) 681–690, http://dx.doi.org/10.1109/TIM.2008.2005259.

[3] L.M. Manojlović, Quadrant photodetector sensitivity, Appl. Opt. 50 (20) (2011) 3461–3469, http://dx.doi.org/10.1364/AO.50.003461.

[4] M. Toyoda, K. Araki, Y. Suzuki, Measurement of the characteristics of a quadrant avalanche photodiode and its application to a laser tracking system, Opt. Eng. 41 (1) (2002) 145–149, http://dx.doi.org/10.1117/1.1418222.

[5] A. Mäkynen, Position-sensitive devices and sensor systems for optical tracking and displacement sensing applications, Department of Electrical Engineering, Oulu University, Oulu, Finland, 2000 (Ph.D. thesis, October 2000).

[6] L. Zhang, Y. Yang, W. Xia, X. Zhu, W. Chen, Y. Lu, Linearity of quadrant avalanche photodiode in laser tracking system, Chin. Opt. Lett. 7 (8) (2009) 728–731.

[7] K.B. Fielhauer, B.G. Boone, J.R. Bruzzi, B.E. Kluga, J.R. Connelly, M.M. Bierbaum, J.J. Gorman, N.G. Dagalakis, Comparison of macro-tip/tilt and mesoscale position beam-steering transducers for free-space optical communications using a quadrant photodiode sensor, in: Proceedings of SPIE, vol. 5160, 2003, pp. 192–203.

[8] E. Akkal, Control actuation systems and seeker units of an air-to-surface guided munition, Middle East Technical University, 2003 (Master's thesis).

[9] S. Donati, C.-Y. Chen, C.-C. Yang, Uncertainty of positioning and displacement measurements in quantum and thermal regimes, IEEE Trans. Instrum. Meas. 56 (5) (2007) 1658–1665, http://dx.doi.org/10.1109/TIM.2007.895584.

[10] A. Marinčić, Ž. Barbarić, Positioning signal analysis of novel quadrant photodiode arrangement, in: Bulletin CXXXVIII, Vol. 31 of Classe des sciences techniques, Academie serbe des sciences et des arts, 2009, pp. 85–90.

[11] X. Hao, C. Kuang, Y. Ku, X. Liu, Y. Li, A quadrant detector based laser alignment method with higher sensitivity, Optik 123 (24) (2012) 2238–2240, http://dx.doi.org/10.1016/j.ijleo.2011.10.031.

[12] E.J. Lee, Y. Park, C.S. Kim, T. Kouh, Detection sensitivity of the optical beam deflection method characterized with the optical spot size on the detector, Curr. Appl. Phys. 10 (3) (2010) 834–837, http://dx.doi.org/10.1016/j.cap.2009.10.003.